Hindawi Publishing Corporation
Journal of Chemistry
Volume 2013, Article ID 258519, 14 pages
http://dx.doi.org/10.1155/2013/258519

Research Article

Molecular Modeling and Spectroscopic Studies of Benzothiazole

V. Sathyanarayanmoorthi,[1] R. Karunathan,[1] and V. Kannappan[2]

[1] *PG and Research Department of Physics, PSG College of Arts and Science, Coimbatore 641 014, India*
[2] *PG and Research Department of Chemistry, Presidency College, Chennai 600 005, India*

Correspondence should be addressed to V. Sathyanarayanmoorthi; sathyanarayanamoorthi@yahoo.co.in

Received 20 May 2013; Revised 23 July 2013; Accepted 26 July 2013

Academic Editor: Cengiz Soykan

The Fourier Transform (FT) infrared and FT-Raman spectra of benzothiazole (BT) have been recorded and analyzed. The equilibrium geometry, bonding features, and harmonic vibrational frequencies have been investigated by ab initio and density functional theory (DFT) methods. The assignments of the vibrational spectra have been carried out. The computed optimized geometric bond lengths and bond angles show good agreement with experimental data of the title compound. The calculated HOMO and LUMO energies indicate that charge transfer occurs within the molecule. Stability of the molecule due to conjugative interactions arising from charge delocalization has been analyzed using natural bond orbital (NBO) analysis. The results show that the electron density (ED) in the σ^* and π^* antibonding orbital and second-order delocalization energies $E(2)$ confirm the occurrence of intramolecular charge transfer (ICT). The calculated results were applied to simulate infrared and Raman spectra BT which show good agreement with recorded spectra.

1. Introduction

Benzothiazole (BT) molecule contains a thiazole ring fused with benzene ring. Thiazole ring is a five-member ring consists of one nitrogen and one sulfur atom in the ring. Benzothiazole is thus a bicyclic aromatic ring system. A number of BT derivatives have been studied as central muscle relaxants and found to interfere with glutamate neurotransmission in biochemical, electrophysiological, and behavioral experiments [1]. Substituted benzothiazoles have been studied and found to have various chemical reactivity and biological activity. Benzothiazole ring is found to possess pharmacological activities such as antiviral [2], antibacterial [3], antimicrobial [4], and fungicidal activities [5]. They are also useful as antiallergic [6], antidiabeticantitumor [7], antitumor [8], anti-inflammatory [9], anthelmintic [10], and anti-HIV agents. Phenyl substituted benzothiazoles show antitumor activity [11–13] while condensed pyrimido benzothiazoles and benzothiazoloquinazolines show antiviral activity. Substituted 6-nitro- and 6-amino-benzothiazoles show antimicrobial activity.

Molecular spectroscopic methods, in particular, experimental IR and Raman spectroscopy, have been successfully employed for structural investigation of complex molecular compounds. These techniques are especially effective when used in combination with direct methods of structural analysis in hydrogen bond investigations. The aim of the present work is theoretical and experimental spectroscopic investigation of BT molecular structure to gain insight into the structure and physical properties of the molecular structure. The FT-IR and FT-Raman spectra were simulated and compared with experimental results. Ab initio and DFT calculations have been performed to support the wave number assignments.

2. Methodology

2.1. Experimental Details. The compound under investigation, namely, BT, is spectral grade purchased from M/S Aldrich Chemicals, USA, and it is used as such without further purification. The FT-IR spectrum of the compound was recorded in Perkin-Elmer Spectrometer in the range of 4000–100 cm^{-1} using KBr pellet technique. The spectral resolution is 0.1 cm^{-1}. The FT-Raman spectrum of the compound was recorded in the BRUKER RFS 27 and Standalone FT-Raman

Spectrometer in the frequency range 50–4000 cm^{-1}. The Laser source is Nd : YAG laser source operating at 1064 nm line with 200 mW power. The spectra were recorded with scanning speed of 20 cm^{-1}. The frequencies of all sharp bands are accurate to ±1 cm^{-1}.

2.2. Computational Details. The molecular geometry optimization and vibrational frequency calculations were carried out on benzothiazole, with GAUSSIAN 09W software package [14] HF functional [15, 16] combined with standard 6-311G and 6-311++G (d, p) basis set (referred to as "large" basis) and the density functional method used is B3LYP, that is, Becke's three-parameter hybrid functional with the Lee-Yang-Parr correlation functional method with 6-311++G (d, p). The harmonic vibrational frequencies calculated for BT at HF and B3LYP levels using the triple split valence basis set along with the diffuse and polarization functions. It may be pointed out that computed wave number corresponds to the isolated molecular state in the gaseous phase whereas the experimental wave numbers correspond to the solid state spectra. In order to evaluate the energetic behavior of the title compound, we carried out calculations in vacuo and in organic solvent (ethanol). The energies of important molecular orbitals of BT, the highest occupied MOs (HOMO), and the lowest unoccupied MOs (LUMO) were calculated using HF/6-311++G (d, p) method. NBO analysis has been performed on the BT molecule at the HF/6-311++G (d, p) and B3LYP/6-311++G (d, p) level in order to elucidate the intramolecular, rehybridization, and delocalization of electron density within the molecule. The result of interaction is a loss of occupancy from the density of electron in NBO of the idealized Lewis structure into an empty non-Lewis orbital. For each donor (i) and acceptor (j), the stabilization energy $E(2)$ associated with the delocalization $i \rightarrow j$ is estimated as

$$E(2) = -n_\sigma \frac{\langle \sigma | F | \sigma \rangle^2}{\varepsilon_\sigma^* - \varepsilon_\sigma} = -n_\sigma \frac{{F_{ij}}^2}{\Delta E}, \quad (1)$$

where $\langle \sigma | F | \sigma \rangle^2$ or ${F_{ij}}^2$ is the Fock matrix element i and j NBO orbital's, ε_σ^* and $-\varepsilon_\sigma$ are the energies of σ and σ^* NBOs, and n_σ is the population of the donor σ orbital. Zero point vibrational energy, internal energy and its translational, rotational, and vibrational contributions, entropy, and heat capacity of BT are computed through the calculation of partition functions [17–19].

3. Results and Discussion

3.1. Molecular Geometry. The optimized geometry of the molecule under investigation with IUPAC numbering scheme for the atoms is presented in Figure 1. The data of structural parameters obtained by ab initio method as compared to density functional theory for benzothiazole are reported in Table 1. The comparative graphs of bond lengths and bond angles of the title molecule are presented in Figure 2. From the computed values, it is found that most of the optimized bond lengths are slightly larger than the experimental values, this may be due to the fact that theoretical calculations

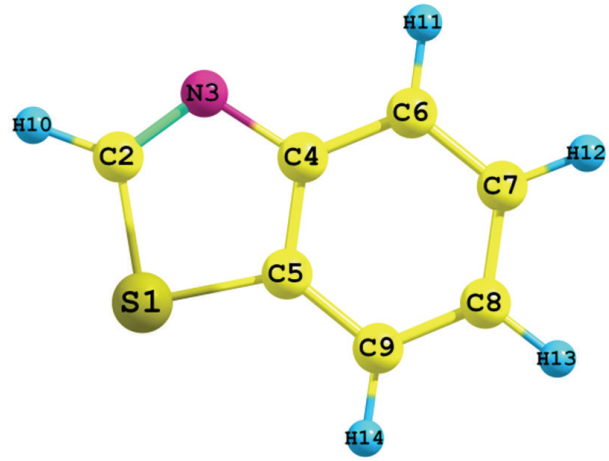

Figure 1: Optimized structure of benzothiazole.

belong to isolated molecules in gaseous phase and the experimental results belong to molecules in solid state. Comparing bond angles and lengths obtained by B3LYP method with those obtained by HF, as a whole the values got by the former are higher than those obtained be the later method. It may be pointed out that the values calculated by B3LYP method correlate satisfactorily with the experimental data. From the data shown in Table 1, it is seen that both HF and DFT (B3LYP/6-311++G (d, p)) levels of theory in general estimate the same values of some bond lengths and bond angles. It is well known that HF methods underestimate and DFT method overestimates bond lengths, particularly the C–H bond lengths [20, 21]. This theoretical pattern is also found for benzothiazole molecule.

The carbon–carbon bonds in benzene are not of equal length which is justified by the presence of fused thiazole ring. However, the differences between the six C–C distances are small. The longest bond distance in C4–C5 bond is due to the fusion of thiazole moiety at these carbons. Comparing the bond distances of the hetero aromatic ring, it is found that the bond distances in hetero aromatic ring differ significantly from each other due to the difference in electronegativities of the bonded atoms. The S1–C2 bond distance is the longest (1.7651 Å) while the C2–N3 is the shortest (1.2874 Å). The longest S1–C2 distance attributes the pure single bond character. The C5–S1 and C2–S1 bond distances of BT determined by B3LYP/6-311++G (d, p) method are 1.75 Å and 1.7651 Å, respectively, in between the 1.81 Å average distance for a carbon–sulfur bond and the 1.61 Å which indicate that the actual bond order is between one and two which is due to conjugative effect in benzothiazole. Due to ring strain the C2–N3 double bond distance is 1.268 Å, 1.268 Å, 1.263 Å in HF, and 1.2874 Å for B3LYP/6-311++G (d, p) bigger than single bond C2–H10. With the electron donating substituents on the benzene ring, the symmetry of the ring is distorted, yielding ring angles smaller than 120° at the point of substitution and slightly larger than 120° at the ortho- and metapositions [22]. It is observed that in BT molecule the bond angle at the point of substitution C4–C5–C9 is 118.7° in HF and 118.9°

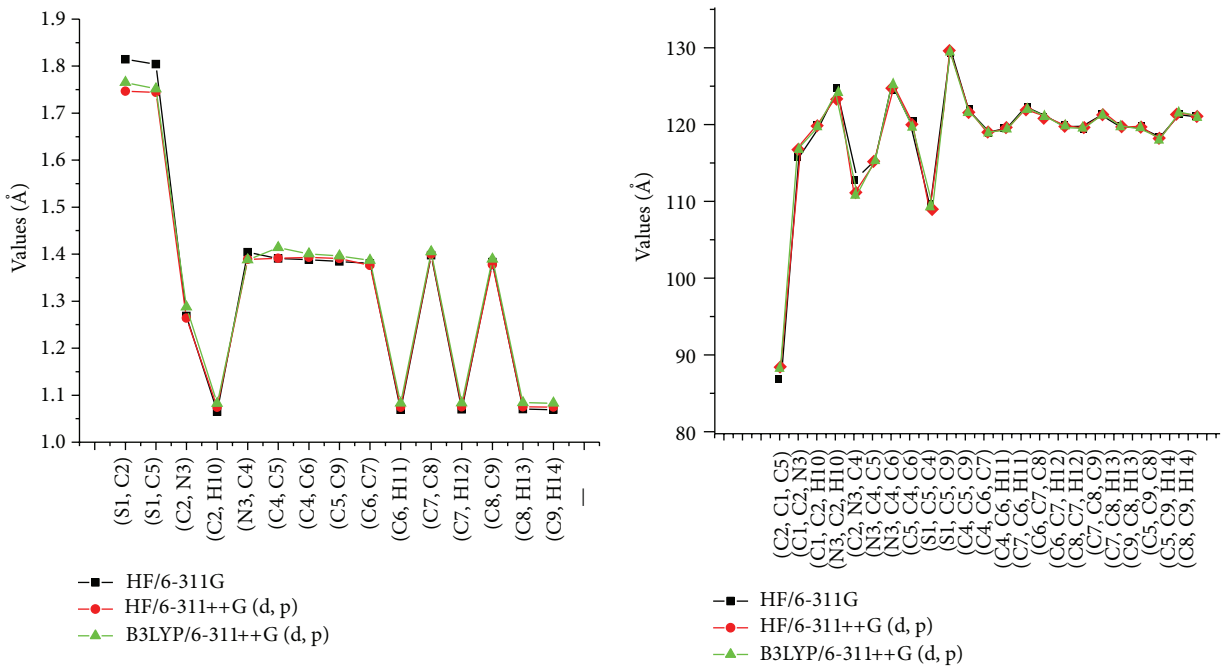

Figure 2: Bond length and bond angle difference between theoretical (HF and DFT) approaches.

in DFT while the bond angles in at ortho to the substituted carbon, C6–C7–C8 position is found to be 120.8677, 120.908 degree at HF and DFT respectively. This may be due to mesomeric effect of the thiazole ring. The meta position angle C7–C8–C9 is greater than 120° and is found to be 120.91°, 121.078°. More distortion in bond parameters is observed in the heteroring than in the benzene ring. The variation in bond angle depends on the electronegativity of the central atom, the presence of lone pair of electrons, and the conjugation of the double bonds. If the electro negativity of the central atom is less, the bond angle decreases. Thus, the bond angle C5–S1–C2 is very less (88.2122°, 88.2011°) than the bond angle C8–N3–C2 (110.755°, 110.742°) which is due to the fact that electronegativity of nitrogen is greater than sulfur.

3.2. Vibrational Assignments. The BT molecule consists of 14 atoms and so it has 36 normal vibrational modes. The observed vibrational assignments and analysis of BT are discussed in terms of fundamental bands. The harmonic vibrational frequencies calculated for BT at HF and B3LYP levels along with the observed FT-IR and FT-Raman frequencies for various modes of vibrations have been presented in Table 2. The comparative values of IR and Raman intensities are given in Table 3. The recorded FT-IR and FT-Raman spectra of BT are given in in Figures 3(a) and 3(b) respectively. Theoretical FT-IR and FT-Raman spectra are reported in Figures 4 and 5, respectively. It may be pointed out here that computed wave numbers correspond to the isolated molecular state in the gas phase whereas the experimental wave numbers correspond to the solid state spectra. The calculated vibrational frequencies using different methods are compared with experimentally observed values. The calculated vibrational wave numbers are consistent with the experimental results. Few bands predicted theoretically in FT-IR spectra were not observed in the experimental spectrum of BT molecule may be due to their very weak intensity.

3.2.1. C–H Stretching. Aromatic compounds commonly exhibit multiple weak bands in the region 3100–3000 cm^{-1} [23–25] due to aromatic C–H stretching vibrations. In the present case, the C–H stretching vibrations are captured at 3061, 3150 cm^{-1} in (mode no. 32, 33) FT-IR spectrum and corresponding Raman spectrum observed at 3063 cm^{-1}. The aromatic C–H in-plane bending modes of benzene and its derivatives are observed in the region 1300–1000 cm^{-1}. The C–H out-of-plane bending modes [26–29] are usually of medium intensity and absorption in the region 950–600 cm^{-1}. In the case of BT, the bands observed at 1069, 1124, 1157, 1198, and 1264 cm^{-1} (mode no. 17, 19, 20, 21, and 22) in IR and at 1292 cm^{-1} in Raman spectra are assigned to the C–H in-plane bending vibrations. The C–H out of plane bending mode of benzene derivatives is observed in the region 1000–600 cm^{-1}. The aromatic C–H out of plane bending vibrations of BT are assigned to the medium to weak bands observed at 1014 and 978 cm^{-1} (mode no. 14, 15) in the infrared spectrum and 1016 cm^{-1} in Raman spectrum. The aromatic C–H in-plane and out of plane bending vibrations have substantial overlapping with the ring C–C–C in-plane and out of plane bending modes, respectively.

3.2.2. C–S Stretching. The C–S and S–H bonds are highly polarizable and hence exhibit stronger spectral activity. The C–S stretching vibration is expected in the region 710–685 cm^{-1} [30]. The C–S stretching vibrations were observed

Table 1: Optimized some geometrical parameters of benzothiazole, bond length (Å), and bond angles (°).

Parameters	HF/6-31G	HF/6-311G	HF/6-311++G	B3LYP/6-311G
Bond length				
(S1, C2)	1.8159	1.8146	1.7464	1.7651
(S1, C5)	1.8096	1.8043	1.7443	1.7518
(C2, N3)	1.2688	1.2683	1.2638	1.2874
(C2, H10)	1.0665	1.0647	1.0744	1.0827
(N3, C4)	1.4031	1.404	1.3886	1.3877
(C4, C5)	1.3926	1.391	1.3912	1.4139
(C4, C6)	1.3887	1.3882	1.3932	1.4008
(C5, C9)	1.385	1.3844	1.3907	1.3962
(C6, C7)	1.3811	1.3803	1.3761	1.3866
(C6, H11)	1.0713	1.0689	1.0743	1.0832
(C7, C8)	1.3975	1.3976	1.3994	1.405
(C7, H12)	1.0723	1.07	1.075	1.0838
(C8, C9)	1.3843	1.383	1.3774	1.3893
(C8, H13)	1.0726	1.0703	1.0751	1.0839
(C9, H14)	1.0715	1.0694	1.0746	1.0832
Bond angle				
(C2, C1, C5)	86.7846	86.8578	88.2122	88.2011
(C1, C2, N3)	115.703	115.6631	116.9227	116.6919
(C1, C2, H10)	119.792	119.7907	119.7167	119.3151
(N3, C2, H10)	124.5047	124.5462	123.3605	123.993
(C2, N3, C4)	112.9102	112.8215	110.755	110.742
(N3, C4, C5)	115.155	115.1091	115.1782	115.2284
(N3, C4, C6)	124.5797	124.5766	124.855	125.1777
(C5, C4, C6)	120.2653	120.3142	119.9668	119.5939
(S1, C5, C4)	109.4469	109.5485	108.9318	109.1366
(S1, C5, C9)	129.1903	129.1251	129.6054	129.4096
(C4, C5, C9)	121.3628	121.3263	121.4628	121.4538
(C4, C6, C7)	118.7264	118.7178	118.7551	118.9556
(C4, C6, H11)	119.3604	119.2699	119.5996	119.307
(C7, C6, H11)	121.9132	122.0123	121.6452	121.7374
(C6, C7, C8)	120.6426	120.6135	120.8677	120.908
(C6, C7, H12)	119.8217	119.8388	119.7498	119.6972
(C8, C7, H12)	119.5357	119.5477	119.3825	119.3948
(C7, C8, C9)	120.9529	120.9354	120.9119	121.0788
(C7, C8, H13)	119.5983	119.6269	119.5658	119.5843
(C9, C8, H13)	119.4487	119.4377	119.5223	119.3369
(C5, C9, C8)	118.0499	118.0927	118.0357	118.0099
(C5, C9, H14)	121.1939	121.1702	121.132	121.2411
(C8, C9, H14)	120.7561	120.7371	120.8323	120.749

in the region 609–716 cm^{-1} for 2-mercapto benzothiazole [31]. The calculated values of the vibrations range from 572 cm^{-1} to 876 cm^{-1}. For 2-mercaptobenzoxazole [32], the calculated values of the vibrations range from 579 cm^{-1} to 892 cm^{-1} and the observed C–S stretching vibration is 954 cm^{-1}. In our title molecule, the C–S stretching is observed at 667 and 799 cm^{-1} (mode no. 9, 11) in FT-IR. The FT-Raman spectrum value at 801 cm^{-1} as a medium band is assigned to C–S stretching vibration. The calculated frequencies of 668, 652, 600, and 626 cm^{-1} exactly correlate with experimental observation as well as the literature data. The C–S vibration is a pure mode as evident from Table 2. The in-plane and out-of-plane C–S stretching vibration also exactly correlates with experimental observations.

3.2.3. C=N Vibrations. The C=N stretching vibrations [33–36] are observed in the range 1672–1566 cm^{-1}. Varsanyi [37] has suggested that an IR band at 1626 cm^{-1} for C=N stretching and Raman frequency is assigned to the C=N stretching vibration of benzothizaole [38]. The respective

Table 2: Comparison of the experimental (FT-IR and FT-Raman) and theoretical harmonic wave numbers (cm^{-1}) of benzothiazole calculated by HF, B3LYP with 6-311++G(d, p) basis set.

Modes no.	Experimental		6-311G	6-311++G	B3LYP 6-311++G	Assignment
	IR	Raman				
1.		71.44	185.6993	221.8993	158.2282	C–H—out of plane bending
2.		210.04	244.1506	259.6877	225.0702	C–H—out of plane bending
3.		352.91	372.6441	373.5584	341.0859	Ring stretching
4.		424.17	426.2948	414.1324	350.0611	N–CH Wagging
5.			471.7758	467.2944	429.3019	C–S–C in plane bending
6.	531	505.08	520.8227	507.0766	451.8357	C–C–C—out of plane bending
7.	585		541.0727	532.2922	481.3446	C–C–C—out of plane bending
8.			623.6493	608.7293	560.6751	C–C–C—out of plane bending
9.	667		668.2929	652.4117	600.4245	C–S Stretching
10.	769	706.88	730.3856	717.6507	666.7194	C–C–C Ring breathing
11.	799	801.01	777.8919	759.172	709.0033	C–S Stretching
12.	828		846.4841	825.1871	754.3702	Thiazole Ring Stretching
13.	873		877.3007	872.0681	804.3435	C–C–C—in plane bending
14.	978		974.2327	929.8297	827.145	C–H—out of plane bending
15.	1014	1015.54	1025.745	970.2269	875.2731	C–H—out of plane bending
16.			1058.5012	1030.8954	922.7485	C–S—Stretching
17.	1069		1085.408	1053.4724	985.3864	C–H—in plane bending
18.			1110.2525	1069.5475	993.4765	C–H—in plane bending
19.	1124	1124.88	1124.8897	1096.4601	1015	C–H—in plane bending
20.	1157		1166.0662	1125.1724	1027.9394	C–H—in plane bending
21.	1198	1197.98	1194.0921	1154.4126	1092.4829	C–H—in plane bending
22.	1264		1203.5496	1178.2819	1126.6974	C–H—in plane bending
23.	1292	1291.66	1243.9149	1216.6827	1153.3509	C–C Stretching
24.	1315	1316.01	1338.3513	1309.6226	1244.4551	C–C—Stretching
25.	1423		1394.2405	1364.2723	1268.7322	C–C—Stretching
26.	1454	1424.58	1427.192	1397.859	1275.7476	C–C—Stretching
27.	1490	1468.87	1575.3975	1556.5462	1440.267	C–H in plane bending
28.	1556	1557.01	1585.4282	1562.2713	1444.1304	C–H in plane bending
29.	1592		1654.5209	1642.2366	1519.1381	C=N Stretching
30.	1657		1663.2985	1653.9474	1535.0676	C–C–C Stretching
31.	1692		1716.6492	1703.8545	1628.1791	C=N Stretching
32.	3061	3063.23	3070.1368	3105.7742	3028.6049	C–H Stretching
33.	3150		3082.2096	3116.571	3036.013	C–H Stretching
34.			3085.3847	3118.2409	3037.4297	C–H Stretching
35.			3094.2296	3126.9054	3046.2331	C–H Stretching
36.			3105.5365	3135.3642	3054.1799	C–H Stretching

bands occurring at 1692 and 1592 cm^{-1} (mode no. 29, 31) in IR spectra is assigned to the C=N stretching vibration for BT molecule. The bands corresponding to the C–C–C and C–S–C in-plane and out of plane bending modes of BT are presented in Table 3. Normal coordinate analysis shows that significant mixing of C–C–C in-plane bending with C–H in-plane bending occurs. Similarly, the skeletal out of plane bending modes are overlapped with C–H out of plane bending modes significantly. The theoretically calculated values of C=N Stretching vibrations are in the region 1717, 1704, and 1629 cm^{-1}.

3.2.4. Ring Vibrations. The carbon–carbon stretching modes of the benzene ring are expected to be in the range from 1650 to 1200 cm^{-1} and are usually not very sensitive to substitution by small substituents, but heavy halogens diminish the frequency [39, 40]. In the Raman spectrum of BT, the carbon–carbon stretching bands appeared at 1596, 1575, 1478, and

Table 3: Comparative values of IR and Raman intensities between HF/6-311G++(d, p) and B3LYP/6-311G++(d, p) of benzothiazole.

HF/6-311G (d, p)		HF/6-311++G (d, p)		B3LYP/6-311++G (d, p)	
IR intensity	Raman intensity	IR intensity	Raman intensity	IR intensity	Raman intensity
8.55	31.44	7.69	16.97	12.75	32.04
0.87	10.21	1.58	7.93	1.23	7.36
1.11	15.00	1.26	14.27	1.19	13.42
14.98	26.31	17.53	25.42	22.89	22.11
1.14	24.06	0.97	16.81	1.513	19.92
12.88	9.86	11.17	7.72	10.50	5.311
0.17	6.11	2.07	3.90	1.79	4.11
6.63	3.63	5.86	3.62	6.73	2.43
3.04	2.78	4.66	2.08	4.05	2.15
4.84	5.27	5.06	5.14	5.06	2.90
16.16	8.09	14.71	9.23	18.48	11.02
20.38	6.69	26.21	3.72	23.66	1.91
14.24	3.81	15.91	3.61	10.31	3.08
88.08	0.38	78.09	4.38	78.12	0.52
11.60	18.23	24.84	13.09	17.20	4.92
12.48	4.88	10.48	10.79	2.23	1.10
15.42	2.25	16.04	6.34	10.29	9.35
0.58	1.192	5.73	2.50	13.25	17.50
12.94	2.06	7.02	1.59	1.43	1.99
3.15	1.57	4.43	1.34	1.70	2.25
2.39	0.65	0.82	0.11	7.34	18.81
3.40	0.08	8.71	3.65	1.30	7.484
12.76	5.03	16.28	9.62	8.45	1.82
1.98	0.18	1.16	0.13	7.05	0.10
0.07	2.50	1.02	2.27	16.98	4.84
34.14	3.30	40.98	3.72	7.68	0.81
27.04	0.98	14.87	1.57	8.36	1.87
6.66	0.87	29.51	0.63	19.58	0.29
10.29	9.44	13.58	13.94	9.66	13.7
16.35	3.27	8.27	2.84	0.99	1.65
98.69	9.45	112.55	19.48	108.78	11.77
0.30	2.40	0.15	1.97	0.06	2.14
7.94	6.26	4.21	5.60	4.37	10.42
13.26	10.55	9.96	9.44	3.21	6.44
23.65	2.74	14.21	2.44	10.14	3.24
23.43	15.30	12.95	13.86	9.55	16.75

1209 cm^{-1}. The corresponding C–C stretching modes are observed in the infrared spectrum at 1454, 1423, 1315, and 1292.31 cm^{-1} (mode no. 23, 24, 25, and 26). The theoretically calculated values are calculated at 1604, 1602, 1486, 1454, 1328, and 1304 cm^{-1} and these values show excellent agreement with experimental data.

The infrared band at 873 cm^{-1} and two Raman bands at 1000 and 700 cm^{-1} (mode no. 13) are assigned to C–C–C in-plane bending vibrations of BT. The C–C in-plane bending vibrations appeared as the combination vibrations with C–H in-plane bending vibrations. The bands assigned to C–C–C out-of-plane bending vibrations are observed at 585, 531 cm^{-1} in (mode no. 6, 7) FTIR spectrum and 505 cm^{-1} in Raman spectrum for BT. The ring breathing vibrations are generally very strong in Raman spectrum. This mode is found in the region 1100–1000 cm^{-1} for a heavy substituted compound and is strongly Raman active. This is confirmed by the very weak intense Raman band at 706 cm^{-1} which is supported by computed results. The ring stretching mode is captured at 372.6441, 373.5584, and 341.0859 cm^{-1} (mode no. 3) in HF/6-311++G (d, p) and B3LYP/6-311++G (d, p) for benzothiazole molecule. Comparison of IR intensities and Raman intensities calculated (Table 3) by HF and DFT (B3LYP) at 6-311+G (d, p) level with experimental values exposes the variation of IR intensities and Raman intensities. Most of the cases, the values of IR intensities by HF are found

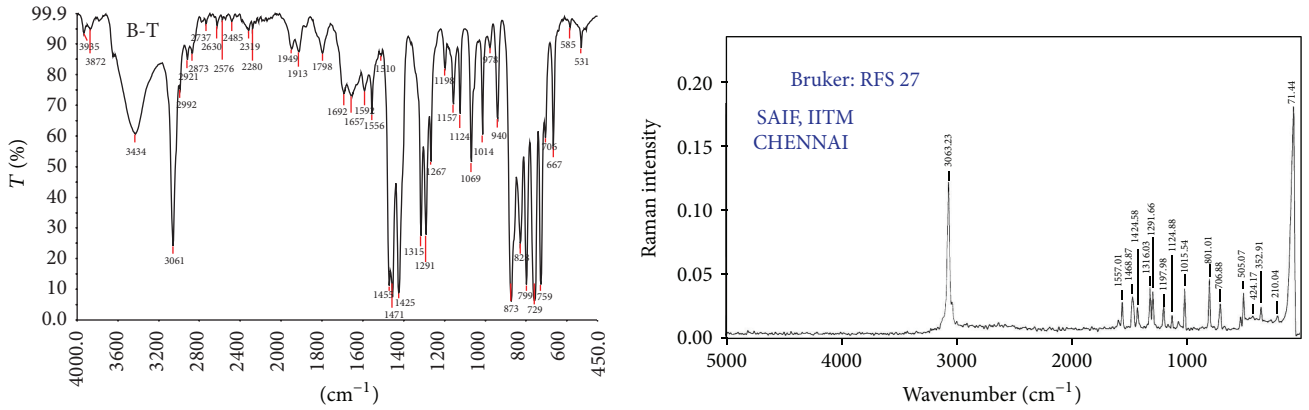

(a) (b)

Figure 3: Experimental FT-IR and FT-Raman spectrum of benzothiazole.

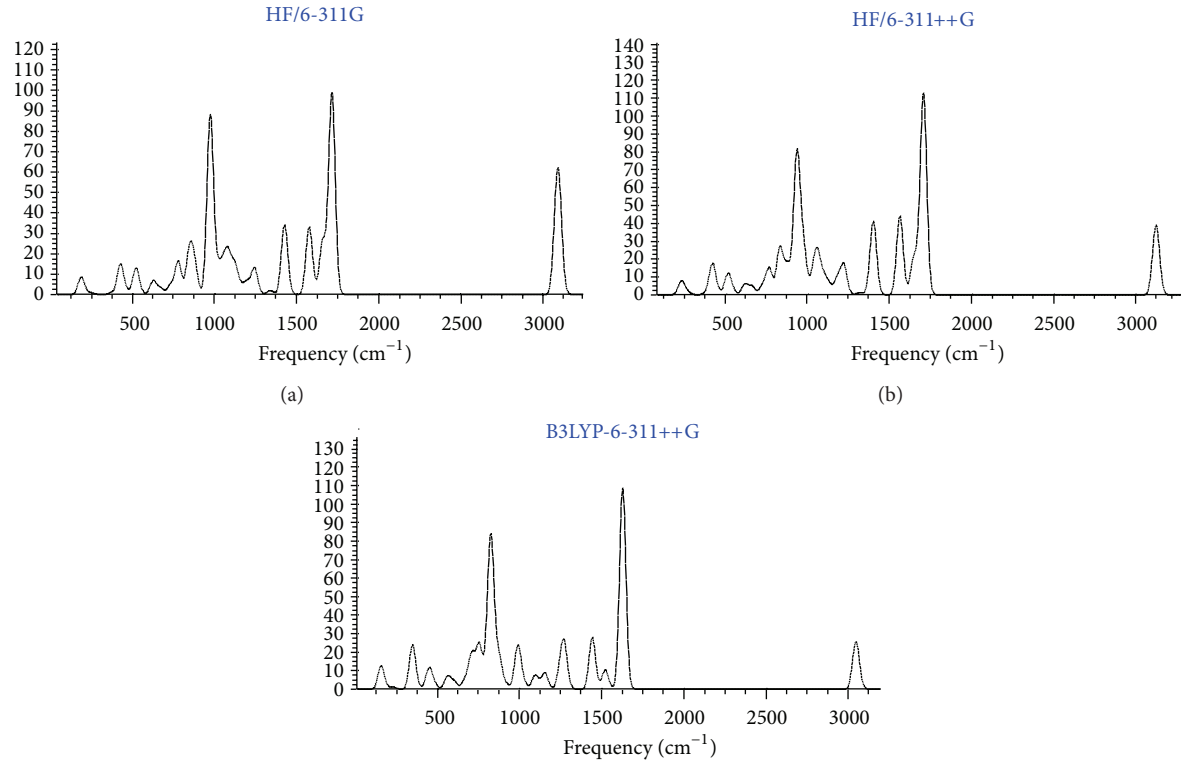

(a) (b) (c)

Figure 4: Theoretical FT-IR spectrum of benzothiazole.

to be higher than B3LYP at 6-311+G (d, p) level whereas in the case of Raman activities the trend is reverse.

3.3. NBO Analysis. The natural bond orbital analysis provides an efficient method for studying intra- and intermolecular bonding and interaction among bonds and also provides a convenient basis for investigating charge transfer or conjugative interaction in molecular systems. Some electron donor orbital, acceptor orbital, and the interacting stabilization energy resulting from the second-order microdisturbance theory are reported [41]. NBO analysis has been performed on the title molecule in order to elucidate the intermolecular, rehybridization, and delocalization of electron density within the molecule, which are presented in Tables 4 and 5. A large diversity of energy values was found. The stronger donor character is shown by the p-type lone pair of the nitrogen atoms. The most important interaction ($n - \sigma^*$) energies, related to the resonance in the molecules, are electron donation from the LP(1)S atoms of the electron donating groups to the antibonding acceptor π^*(C–N) of the phenyl

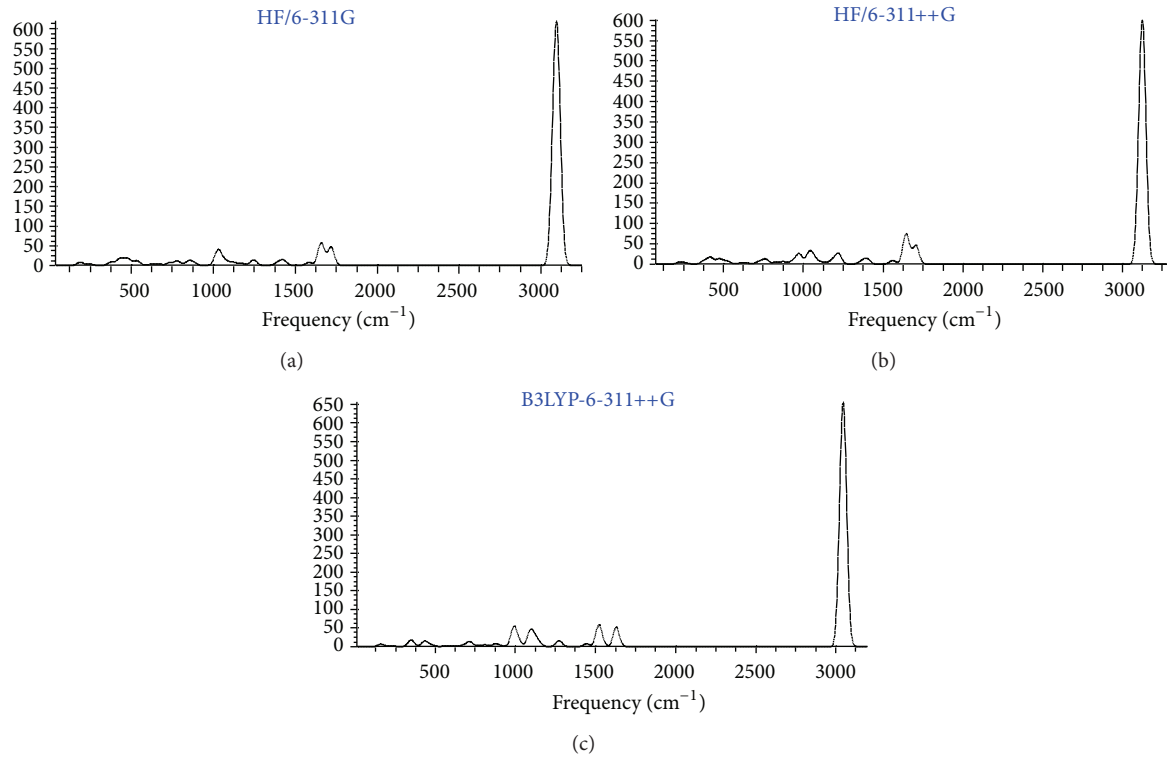

Figure 5: Theoretical FT-Raman spectrum of benzothiazole.

ring LP(1) S1 $\rightarrow$ σ^* (C2–N3) = 1.50 kJ mol^{-1}. This larger energy shows the hyperconjugation between the electron do nating groups and the phenyl ring. NBO analysis has been performed on the BT at the HF/6-11++G (d, p) and DFT level in order to elucidate the intramolecular, rehybridization, and delocalization of electron density within the molecule. The intramolecular interactions are formed by the orbital overlap between bonding (C–C) and (C–C) antibond orbital which results in intramolecular charge transfer (IC T) causing stabilization of the system. These interactions are observed as increase in electron density (ED) in C–C antibonding orbital that weakens the respective bonds. The strong intramolecular conjugative interaction of the σ electron of (S1–C2) distribute to σ^* (S1–C2), C4–C5, C4–C6, and C5–C9 of the ring. On the other hand, the π (C2–N3) in the ring conjugate to the antibonding orbital of π^* (C4–C6) leads to strong delocalization of 18.48 kJ/mol. The π (C4–C6) bond is interacting with π^* (C2–N3) with the energy 12.45 kcal/mol for BT. The σ (C4–C5) bond is interacting with σ^* (C2–H10), σ^* (C4–C6), σ^* (C5–C9), σ^* (C6–H11), σ^* (C9–H14) with the energies 0.68, 5.03, 5.14, 2.13, 2.37 kcal/mol for BT. The energy vlaues of MOs of benzene ring σ (C4–C6, C6–C7, C7–C8, C8–C9), π (C9–C5) are respectively 4.16, 4.51, 2.83, 5.69, 3.79 kcal/mol for BT.

3.4. Frontier Molecular Orbitals (FMOs). The highest occupied molecular orbitals (HOMOs) and the lowest-lying unoccupied molecular orbitals (LUMOs) are called frontier molecular orbital's (FMOs). The FMOs play an important role in the optical and electric properties, as well as in quantum chemistry and UV-vis spectra [37]. The HOMO represents the ability to donate an electron; LUMO as an electron acceptor represents the ability to obtain an electron. The energy gap between HOMO and LUMO determines the kinetic stability, chemical reactivity, and optical polarizability and chemical hardness-softness of a molecule [42, 43].

In order to evaluate the energetic behavior of the title compound, we carried out calculations in vacuo and in organic solvent (ethanol). The energies of important molecular orbitals of BT, the highest occupied MOs (HOMO) the lowest unoccupied MOs (LUMO) were calculated using HF/6-311++G (d, p). The energy values of HOMO and LUMO are −0.2449, −0.05227, respectively. The 3D plots of the HOMO, LUMO orbitals computed for BT molecule are illustrated in Figure 6. The positive phase is red and the negative one is green. It is evident from the figure that while the HOMO is localized on almost the whole molecule, LUMO is localized on the thiazole ring. Both the HOMOs and the LUMOs are mostly π antibonding type orbitals. The calculated energy value of HOMO is −6.4099 eV and LUMO is −2.038 eV, respectively. The energy separation between the HOMO and the LUMO is −4.4061 eV, respectively. The energy gap of HOMO-LUMO explains the eventual charge transfer interaction within the molecule, which influences the biological activity. The wavelength of maximum absorption, excitation energies E (eV), and oscillator strengths (f) of benzothiazole are calculated and given in Table 6. Figure 7 contains theoretically deduced UV-vis spectrum of BT in ethanol employing the TD-HF/6-311++G (d, p) method.

Table 4: Second-order perturbation theory analysis of Fock matrix in NBO basis for benzothiazole.

Donor (i)	Type	ED/e	Acceptor (j)	Type	ED/e	$E(2)$	$E(j) - E(i)^b$ (a. u.)	$F(i, j)^c$ (a. u.)
S1–C2	σ	1.97599	S1–C2	σ^*	0.07093	0.70	0.92	0.023
			C4–C5	σ^*	0.03211	0.78	1.46	0.030
			C4–C6	σ^*	0.02151	1.04	1.50	0.035
			C5–C9	σ^*	0.02268	5.97	1.49	0.084
			C5–C9	π^*	0.35040	3.63	0.84	0.054
S1–C5	σ	1.97203	C2–N3	π^*	0.07212	1.82	0.96	0.038
			C2–H10	σ^*	0.02234	2.59	1.46	0.055
			C5–C9	σ^*	0.02268	0.72	1.54	0.030
			C8–C9	σ^*	0.01365	2.97	1.55	0.061
C2–N3	σ	1.99261	C2–H10	σ^*	0.02234	1.26	1.90	0.044
			N3–C4	σ^*	0.02497	0.94	1.77	0.037
			C4–C6	σ^*	0.02151	3.53	1.99	0.075
			C4–C6	π^*	0.34604	0.80	1.34	0.032
C2–N3	π	1.95466	N3–C4	σ^*	0.02497	1.36	1.07	0.034
			C4–C6	π^*	0.34604	18.48	0.64	0.106
C2–H10	σ	1.98286	C2–N3	σ^*	0.01757	1.83	1.60	0.048
			N3–C4	σ^*	0.02497	8.01	1.33	0.092
N3–C4	σ	1.97560	S1–C2	σ^*	0.07093	1.12	1.15	0.032
			C2–H10	σ^*	0.02234	7.02	1.64	0.096
			C4–C5	σ^*	0.03211	0.54	1.69	0.027
			C4–C6	σ^*	0.02151	1.23	1.73	0.041
			C5–C9	σ^*	0.02268	2.69	1.73	0.061
			C6–C7	σ^*	0.01185	1.80	1.74	0.050
C4–C5	σ	1.97874	C2–H10	σ^*	0.02234	0.68	1.65	0.030
			C4–C6	σ^*	0.02151	5.03	1.74	0.084
			C5–C9	σ^*	0.02268	5.14	1.74	0.084
			C6–H11	σ^*	0.00915	2.13	1.66	0.053
			C9–H14	σ^*	0.01004	2.37	1.66	0.056
C4–C6	σ	1.97510	S1–C5	σ^*	0.01756	4.16	1.22	0.064
			C2–N3	σ^*	0.01757	1.50	1.76	0.046
			C2–N3	π^*	0.07212	0.53	1.12	0.022
			N3–C4	σ^*	0.02497	1.34	1.50	0.040
			C4–C5	σ^*	0.03211	5.54	1.68	0.086
			C6–C7	σ^*	0.01185	2.72	1.72	0.061
			C6–H11	σ^*	0.00915	1.69	1.64	0.047
			C7–H12	σ^*	0.00908	2.25	1.64	0.054
C4–C6	π	1.66368	C2–N3	π^*	0.07212	12.45	0.52	0.077
			N3–C4	σ^*	0.02497	0.94	0.90	0.028
			C5–C9	π^*	0.35040	39.19	0.46	0.120
			C7–C8	π^*	0.32093	39.20	0.47	0.122
C5–C9	σ	1.98148	N3–C4	σ^*	0.02497	3.01	1.52	0.060
			C4–C5	σ^*	0.03211	5.38	1.70	0.086
			C8–C9	σ^*	0.01365	3.05	1.74	0.065
			C8–H13	σ^*	0.00886	2.08	1.65	0.052
			C9–H14	σ^*	0.01004	1.87	1.65	0.050
C5–C9	π	1.70971	C2–N3	π^*	0.07212	1.23	0.54	0.024
			N3–C4	σ^*	0.02497	0.92	0.92	0.028
			C4–C6	π^*	0.34604	36.07	0.48	0.120
			C7–C8	π^*	0.32093	35.76	0.49	0.120

Table 4: Continued.

Donor (i)	Type	ED/e	Acceptor (j)	Type	ED/e	$E(2)$	$E(j) - E(i)^b$ (a. u.)	$F(i, j)^c$ (a. u.)
C6–C7	σ	1.98054	N3–C4	σ^*	0.02497	4.51	1.49	0.07
			C4–C6	σ^*	0.02151	3.29	1.71	0.067
			C6–H11	σ^*	0.00915	1.53	1.63	0.045
			C7–C8	σ^*	0.01359	2.85	1.71	0.062
			C7–H12	σ^*	0.00908	1.44	1.63	0.043
			C8–H13	σ^*	0.00886	2.56	1.62	0.058
C6–H11	σ	1.98222	N3–C4	σ^*	0.02497	0.55	1.28	0.024
			C4–C5	σ^*	0.03211	5.08	1.46	0.077
			C4–C6	σ^*	0.02151	1.42	1.50	0.041
			C6–C7	σ^*	0.01185	1.33	1.50	0.040
			C7–C8	σ^*	0.01359	4.20	1.50	0.071
C7–C8	σ	1.98272	C6–C7	σ^*	0.01185	2.83	1.71	0.062
			C6–H11	σ^*	0.00915	2.48	1.63	0.057
			C7–H12	σ^*	0.00908	1.55	1.63	0.045
			C8–C9	σ^*	0.01365	2.90	1.71	0.063
			C8–H13	σ^*	0.00886	1.56	1.62	0.045
			C9–H14	σ^*	0.01004	2.59	1.62	0.058
C7–C8	π	1.67584	C4–C6	π^*	0.34604	42.89	0.46	0.126
			C5–C9	π^*	0.35040	42.80	0.45	0.125
C7–H12	σ	1.98449	C4–C6	σ^*	0.02151	4.40	1.50	0.073
			C6–C7	σ^*	0.01185	1.28	1.50	0.039
			C7–C8	σ^*	0.01359	1.29	1.50	0.039
			C8–C9	σ^*	0.01365	4.20	1.50	0.071
C8–C9	σ	1.97778	S1–C5	σ^*	0.01756	5.69	1.21	0.074
			C5–C9	σ^*	0.02268	3.97	1.70	0.073
			C7–C8	σ^*	0.01359	2.83	1.71	0.062
			C7–H12	σ^*	0.00908	2.51	1.63	0.057
			C8–H13	σ^*	0.00886	1.43	1.63	0.043
			C9–H14	σ^*	0.01004	1.53	1.62	0.045
C8–H13	σ	1.98412	C5–C9	σ^*	0.02268	4.70	1.49	0.075
			C6–C7	σ^*	0.01185	4.16	1.50	0.071
			C7–C8	σ^*	0.01359	1.29	1.50	0.039
			C8–C9	σ^*	0.01365	1.26	1.50	0.039
C9–H14	σ	1.98424	C4–C5	σ^*	0.03211	4.44	1.46	0.072
			C5–C9	σ^*	0.02268	1.54	1.49	0.043
			C7–C8	σ^*	0.01359	4.07	1.50	0.070
			C8–C9	σ^*	0.01365	1.33	1.50	0.040
C4–C6	π^*	0.34604	C2–N3	π^*	0.07212	18.62	0.05	0.062
			N3–C4	σ^*	0.02497	2.79	0.43	0.072
C5–C9	π^*	0.35040	C2–N3	π^*	0.07212	3.79	0.06	0.030
			C7–C8	π^*	0.32093	371.30	0.02	0.122

[a] $E(2)$ means energy of hyperconjugative interaction (stabilization energy).
[b] Energy difference between donor and acceptor i and j NBO orbitals.
[c] $F(i, j)$ is the Fock matrix element between i and j NBO orbitals.

3.5. Thermodynamic Properties. The values of thermodynamic parameters zero point vibrational energy, thermal energy, specific heat capacity, rotational constants, entropy of BT at 298.15 K in ground state are listed in Table 7. The variation in zero point vibrational energies (ZPVEs) seems to be significant. The ZPVE is much lower by the DFT/B3LYP method than by the HF method. The high value of ZPVE of BT is 65.51 kcl/mol obtained at HF/6-311++G (d, p) whereas the smallest values is 61.63 kcal/mol obtained at B3LYP/6-311++G (d, p). Dipole moment reflects the molecular charge distribution and is given as a vector in three dimensions. Therefore, it can be used as descriptor to depict the charge movement across the molecule. Direction of the dipole moment vector in a molecule depends on the centers of

Table 5: Second-order perturbation energies $E(2)$ (donor → acceptor) for benzothiazole.

Donor (i)	Acceptor (j)	$E(2)$ (kJ mol^{-1})[a]	$E(j) - E(i)$[b] (a. u.)	$F(i, j)$[c] (a. u.)
Within unit 1				
LP (1) S1	σ^*C2–N3	1.50	1.70	0.045
LP (1) S1	π^*C2–N3	1.38	1.05	0.035
LP (1) S1	σ^*C4–C5	1.77	1.61	0.048
LP (1) S1	σ^*C5–C9	0.52	1.64	0.026
LP (2) S1	π^*C2–N3	8.98	0.59	0.065
LP (2) S1	σ^*C2–H10	1.41	1.09	0.036
LP (2) S1	σ^*C4–C5	1.21	1.14	0.034
LP (2) S1	σ^*C5–C9	1.98	1.18	0.044
LP (1) N3	σ^*C2–N6	2.64	1.17	0.050
LP (1) N3	σ^*C4–C5	9.23	1.38	0.102
LP (1) N3	σ^*C4–H7	3.47	1.25	0.060
LP (1) N3	σ^*S1–C2	27.32	0.77	0.130
LP (1) N3	σ^*C4–C6	0.85	1.35	0.031
LP (1) N3	σ^*C4–C6	1.17	0.70	0.027

[a]$E(2)$ means energy of hyper conjugative interaction (stabilization energy).
[b]Energy difference between donor and acceptor i and j NBO orbitals.
[c]$F(i, j)$ is the Fock matrix element between i and j NBO orbitals.

Table 6: Calculated absorption wavelength (nm), excitation energies E (eV), and oscillator strengths (f) of benzothiazole.

TD-HF/6-311++G (d, p) Ethanol			TD-HF/6-311++G (d, p) Gas phase		
λ (mn)	(f)	E (eV)	λ (mn)	(f)	E (eV)
308.1	0.0333	4.0241 eV	308.66	0.0265	4.0169 eV
265.01	0.0013	4.6784 eV	267.95	0.001	4.6272 eV
252.77	0.0025	4.9051 eV	254.78	0.0018	4.8663 eV

Table 7: The calculated thermodynamical parameter of benzothiazole.

Basis Set	HF/6-31G	HF/6-311G	HF/6-311++G (d, p)	B3LYP/6-311++G (d, p)
Zero point energy (Kcal/Mol)	66.93709	66.140	65.51671	61.63
Rotational constant	2.93435	2.93435	2.93435	2.93435
Rotational temperature	0.14083	0.14083	0.14083	0.14083
Energy (E)				
Translational	0.889	0.889	0.889	0.889
Rotational	0.889	0.889	0.889	0.889
Vibrational	68.158	68.168	67.551	64.058
Total	**70.689**	**69.988**	**69.329**	**65.836**
Specific heat (C_v)				
Translational	2.981	2.981	2.981	2.981
Rotational	2.981	2.981	2.981	2.981
Vibrational	17.963	17.973	18.512	15.283
Total	**23.627**	**23.935**	**20.895**	**21.245**
Entropy (S)				
Translational	40.613	40.613	40.613	40.613
Rotational	28.903	28.903	28.903	28.903
Vibrational	10.154	10.167	10.040	12.445
Total	**79.436**	**79.683**	**79.556**	**81.961**
Dipole moment	2.0974	2.0507	1.6331	1.4713

Table 8: Mulliken atomic charges of benzothiazole.

Atoms	HF/6-31G	HF/6-311G	HF/6-311++G (d, p)	B3LYP/6-311++G (d,p)
S1	0.494254	0.283343	−0.428958	−0.305656
C2	−0.223616	−0.09723	−0.1285	−0.174194
N3	−0.43924	−0.377701	0.038389	0.055788
C4	0.177233	0.264898	−0.932014	−0.938592
C5	−0.403325	−0.453121	1.000645	0.984567
C6	−0.120432	−0.09318	−0.43895	−0.437759
C7	−0.221659	−0.167237	−0.377287	−0.307896
C8	−0.184873	−0.165775	−0.246147	−0.081338
C9	−0.19687	−0.144593	0.313292	0.218011
H10	0.242781	0.218665	0.275732	0.255925
H11	0.235255	0.192916	0.244504	0.193902
H12	0.209181	0.176608	0.217394	0.172514
H13	0.207899	0.178898	0.216713	0.174776
H14	0.223413	0.18351	0.245187	0.189952

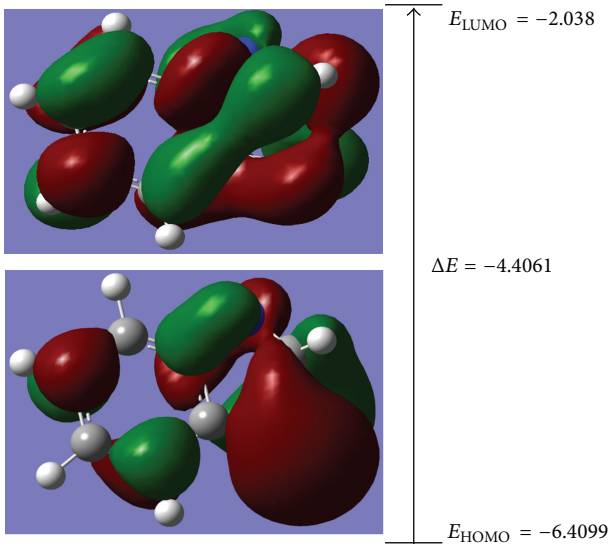

Figure 6: The molecular orbitals and energies for the HOMO and LUMO of the title compound.

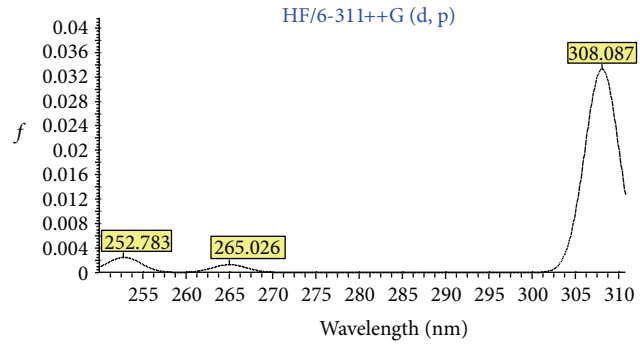

Figure 7: Theoretical UV-vis spectrum in ethanol for the title molecule calculated with the TD-HF/6-311++G (d, p) method.

positive and negative charges. Dipole moments are strictly determined for neutral molecules. For charged systems, its value depends on the choice of origin and molecular orientation. As a result of HF and DFT (B3LYP) calculations, the highest dipole moment was observed for B3LYP/6-311G++(d,p) whereas the smallest one was observed for HF/6-311++G (d, p) in each molecule.

On the basis of vibrational analysis, the statically thermodynamic functions: heat capacity (C), entropy (S), and enthalpy changes (DH) for the title molecule were obtained from the theoretical harmonic frequencies and listed in Table 7. From the data in this table, it can be observed that these thermodynamic functions are increasing with temperature ranging from 100 to 600 K due to the fact that the molecular vibrational intensities increase with temperature [44].

3.6. Mulliken Atomic Charges. Mulliken atomic charge calculation is an important tool in the application of quantum chemical calculation to molecular system because atomic charges influence dipole moment, molecular polarizability, electronic structure, and other physical properties of molecular systems. The calculated Mulliken charge values are listed in Table 8. The atomic charge depends on basis set presumably occur due to polarization. For example, the charge of N (3) atom is −0.43924 for HF/6-31G, −0.377701 for HF/6-311G, 0.038389 for HF/6-311++G (d, p), and 0.055788 for B3LYP/6-311++G (d, p). The charge distribution of sulfur group is increasing trend in HF and B3LYP methods. The charge of H10, H11, H12, H13, and H14 is positive in both HF and DFT diffuse functions. Considering all methods and basis sets used in the atomic charge calculation, the carbon atoms exhibit a substatantial negative charge, which are donor atoms. Hydrogen atom exhibits a positive charge, which is an acceptor atom. The Mulliken charge distribution of BT is increasing trend in B3LYP as compared to HF methods. A comparison of Mullikan's Atomic charge obtained by the two theoretical (HF and DFT) approaches is illustrated in Figure 8. It may be seen that the two methods give comparable atomic charges.

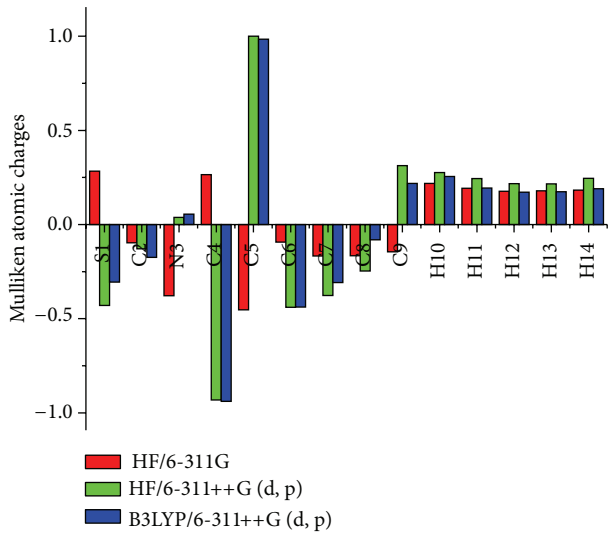

Figure 8: Mullikan's atomic charges between theoretical (HF and DFT) approaches.

4. Conclusion

In the present work, we have performed the experimental and theoretical vibrational analysis of a pharmaceutically important heterocyclic aromatic molecule, benzothiazole for the first time. The optimized molecular geometry, vibrational frequencies, infrared activities, and Raman scattering activities of the molecule in the ground state have been calculated by using ab initio HF and DFT (B3LYP) methods with 6–311++G (d, p) basis set. The vibrational frequencies were calculated and scaled values are compared with the recorded FT-IR and FT-Raman spectra of the compound. The observed and the calculated frequencies are found to be in good agreement. Furthermore, the thermodynamic and total dipole moment properties of the compound have been calculated in order to get insight into molecular structure of the compound. These computations are carried out with the main aim that the results will be of assistance in the quest of the experimental and theoretical evidence for the title molecule in biological activity and coordination chemistry.

References

[1] H. M. Bryson, B. Fulton, and P. Benfield, "Riluzole. A review of its pharmacodynamic and pharmacokinetic properties and therapeutic potential in amyotrophic lateral sclerosis," *Drugs*, vol. 52, no. 4, pp. 549–563, 1996.

[2] S. Akihama, M. Okhude, and A. Mizno, *Chemical Abstracts*, vol. 68, p. 10369v, 1968.

[3] F. Russo and M. Santagati, "Synthesis and determination of the antibacterial activity of benzothiazole derivatives of 1,3,4 thiadiazole and imidazo [2,1 b]1,3,4 thiadiazole," *Farmaco*, vol. 31, no. 1, pp. 41–48, 1976 (Italian).

[4] K. M. Ghoneim, S. El-Basil, A. N. Osman, M. M. Said, and S. A. Megahed, "Synthesis and antimicrobial investigation of benzothiazole derivatives," *Revue Roumaine de Chimie*, vol. 36, pp. 1355–1361, 1991.

[5] S. P. Singh and S. Seghal, "Study of fungicidal activities of some benzothiazoles," *Indian Journal of Chemistry B*, vol. 27, p. 941, 1988.

[6] J. H. Musser, R. E. Brown, B. Love et al., "Synthesis of 2-(2,3-dihydro-2-oxo-1,3,4-oxadiazol-5-yl) benzo heterocycles. A novel series of orally active antiallergic agents," *Journal of Medicinal Chemistry*, vol. 27, pp. 121–125, 1984.

[7] S. R. Pattan, C. Suresh, V. D. Pujar, V. V. K. Reddy, V. P. Rasal, and B. C. Kotti, "Synthesis and antidiabetic activity of 2-amino [5′(4-sulphonylbenzylidine)-2,4-thiazolidinedione]-7-chloro-6-fluorobenzothiazole," *Indian Journal of Chemistry B*, vol. 44, no. 11, pp. 2404–2408, 2005.

[8] M. Yoshida, I. Hayakawa, N. Hyashi et al., "Synthesis and biological evaluation of benzothiazole derivatives as potent antitumor agents," *Bioorganic & Medicinal Chemistry Letters*, vol. 15, pp. 3328–3332, 2005.

[9] S. N. Sawhney, R. K. Tomer, O. M. Prakash, I. Prakash, and S. P. Singh, "Benzothiazole derivatives: Part XI-Synthesis and anti-inflammatory activity of some 2-(3′-5′-dimethyl-4′-substituted-pyrazole-1′-yl) benzothiazoles," *Indian Journal of Chemistry B*, vol. 20, pp. 314–316, 1981.

[10] H. D. Brown, *Chemical Abstracts*, vol. 65, p. 18593, 1966.

[11] C. O. Leong, M. Gaskell, G. A. Martin et al., "Antitumour 2-(4-aminophenyl)benzothiazoles generate DNA adducts in sensitive tumour cells *in vitro* and *in vivo*," *British Journal of Cancer*, vol. 88, pp. 470–477, 2003.

[12] T. D. Bradshaw, M. C. Bibby, J. A. Double et al., "Preclinical evaluation of amino acid prodrugs of novel antitumor 2-(4-amino-3-methylphenyl)benzothiazoles," *Molecular Cancer Therapeutics*, vol. 1, no. 4, pp. 239–246, 2002.

[13] I. Hutchinson, S. A. Jennings, B. R. Vishnuvajjala, A. D. Westwell, and M. F. G. Stevens, "Antitumor benzothiazoles. 16. Synthesis and pharmaceutical properties of antitumor 2-(4-aminophenyl)benzothiazole amino acid prodrugs," *Journal of Medicinal Chemistry*, vol. 45, no. 3, pp. 744–747, 2002.

[14] J. Frisch, G. W. Trucks, H. B. Schlegel et al., *Gaussian 09 Program, Revision C. 01*, Gaussian, Inc, Wallingford, Conn, USA, 2010.

[15] A. D. Becke, "Density-functional thermochemistry. III. The role of exact exchange," *The Journal of Chemical Physics*, vol. 98, no. 7, pp. 5648–5652, 1993.

[16] G. Rauhut and P. Pulay, "Transferable scaling factors for density functional derived vibrational force fields," *The Journal of Physical Chemistry*, vol. 99, no. 10, pp. 3093–3100, 1995.

[17] S. Srinivasan, S. Gunasekaran, U. Ponnambalam, A. Savarianandam, S. Gnanaprakasam, and S. Natarajan, "Spectroscopic and thermodynamic analysis of enolic form of 3-oxo-L-gulofuranolactone," *Indian Journal of Pure and Applied Physics*, vol. 43, no. 6, pp. 459–462, 2005.

[18] G. Socretes, *Infrared Characteristic Group Frequencies*, John Wiley & Sons, New York, NY, USA, 1st edition, 1980.

[19] D. Alfè, G. A. De Wijs, G. Kresse, and M. J. Gillan, "Recent developments in ab initio thermodynamics," *International Journal of Quantum Chemistry*, vol. 77, no. 5, pp. 871–879, 2000.

[20] H. M. Badawi, W. Forner, and Y. S. Oloriegbe, "Theoretical vibrational spectra and potential scans for trichloromethylsulfonyl isocyanate," *Journal of Molecular Structure*, vol. 548, no. 1–3, pp. 219–227, 2001.

[21] D. Mahadevan, S. Periandy, and S. Ramalingam, "FT-IR and FT-Raman, vibrational assignments, molecular geometry, ab initio (HF) and DFT (B3LYP) calculations for 1,3-dichlorobenzene," *Spectrochimica Acta A*, vol. 79, no. 5, pp. 962–969, 2011.

[22] M. Batley, R. Bramley, and K. Robinson, "Photophysics of the lowest triplet state in 2-benzoylpyridine crystals. I. Optical spectra," *Proceedings of the Royal Society A*, vol. 369, pp. 175–185, 1979.

[23] Y. Wang, S. Saebo, and C. U. Pittman Jr., "The structure of aniline by ab initio studies," *Journal of Molecular Structure*, vol. 281, no. 2-3, pp. 91–98, 1993.

[24] I. Fleming, *Frontier Orbitals and Organic Chemical Reactions*, John Wiley & Sons, London, UK, 1976.

[25] A. M. Asiri, M. Karabacak, M. Kurt, and K. A. Alamry, "Synthesis, molecular conformation, vibrational and electronic transition, isometric chemical shift, polarizability and hyperpolarizability analysis of 3-(4-methoxy-phenyl)-2-(4-nitro-phenyl)-acrylonitrile: a combined experimental and theoretical analysis," *Spectrochim Acta A*, vol. 82, pp. 444–455, 2011.

[26] B. Kosar and C. Albayrak, "Spectroscopic investigations and quantum chemical computational study of (E)-4-methoxy-2-[(p-tolylimino)methyl]phenol," *Spectrochimica Acta A*, vol. 78, no. 1, pp. 160–167, 2011.

[27] A. A. El-Azhary, "A DFT study of the geometries and vibrational spectra of indene and some of its heterocyclic analogues, benzofuran, benzoxazole, bensothiophene, benzothiazole, indole and indazole," *Spectrochim Acta A*, vol. 55, no. 12, pp. 2437–2446, 1999.

[28] Y. Wang, S. Saebo, and C. U. Pittman Jr, "The structure of aniline by ab initio studies," *Journal of Molecular Structure*, vol. 281, no. 2-3, pp. 91–98, 1993.

[29] A. Altun, K. Gölcük, and M. Kumru, "Structure and vibrational spectra of p-methylaniline: Hartree-Fock, MP2 and density functional theory studies," *Journal of Molecular Structure*, vol. 637, pp. 155–169, 2003.

[30] J. Coates, *Interpretation of Infrared Spectra, A Practical Approach*, John Wiley & Sons, Chichester, UK, 2000.

[31] X. Li, Z. Tang, and X. Zhang, "Molecular structure, IR spectra of 2-mercaptobenzothiazole and 2-mercaptobenzoxazole by density functional theory and ab initio Hartree-Fock calculations ," *Spectrochim Acta A*, vol. 74, no. 1, pp. 168–173, 2009.

[32] I. Yalcin, E. Sener, T. Ozden, S. Ozden, and A. Akin, "Synthesis and microbiological activity of 5-methyl-2-[p-substituted phenyl]benzoxazoles," *European Journal of Medicinal Chemistry*, vol. 25, no. 8, pp. 705–708, 1990.

[33] R. Saxena, L. D. Kandpal, and G. N. Mathur, "Synthesis and characterization of poly(benzobisthiazole)s derived from halogenated phthalic acid and isophthalic acid," *Journal of Polymer Science A*, vol. 40, no. 22, pp. 3959–3966, 2002.

[34] R. M. Silverstein, G. C. Bassler, and T. C. Morril, *Spectrometric Identification of Organic Compounds*, John Wiley & Sons, Singapore, 5th edition, 1991.

[35] K. Nakamoto, *Infrared and Raman Spectrum of Inorganic and Coordination Compounds*, John Wiley & Sons, NewYork, NY, USA, 5th edition, 1997.

[36] G. Yang, S. I. Matsuzono, E. Koyama, H. Tokuhisa, and K. Hiratani, "A new synthetic route to benzoxazole polymer via tandem claisen rearrangement," *Macromolecules*, vol. 34, no. 19, pp. 6545–6547, 2001.

[37] G. Varsanyi, *Assignments for Vibrational Spectra of Seven Hundred Benzene Derivatives*, vol. 1, Adam Hilger, London, UK, 1974.

[38] G. Socrates, *Infrared Raman Characteristic Group Frequencies—Tables and Charts*, John Wiley & Sons, New York, NY, USA, 3rd edition, 2001.

[39] V. Krishnakumar and R. J. Xavier, "Normal coordinate analysis of 2-mercapto and 4,6-dihydroxy-2-mercapto pyrimidines," *Indian Journal of Pure and Applied Physics*, vol. 41, pp. 597–601, 2003.

[40] J. N. Liu, Z. R. Chen, and S. F. Yuan, "Study on the prediction of visible absorption maxima of azobenzene compounds," *Journal of Zhejiang University Science B*, vol. 6, pp. 584–589, 2005.

[41] R. Zhang, B. Dub, G. Sun, and Y. Sun, "Experimental and theoretical studies on *o*-, *m*- and *p*-chlorobenzylideneamino-antipyrines," *Spectrochimica Acta A*, vol. 75, pp. 1115–1124, 2010.

[42] L. J. Bellamy, *The Infrared Spectra of Complex Molecules*, John Wiley & Sons, NewYork, NY, USA, 3rd edition, 1975.

[43] E. Koglin, E. G. Witte, and R. J. Meier, "The vibrational spectra of metabolites of methabenzthiazuron: 2-amino-benzothiazole and 2-(methylamino)benzothiazole," *Vibrational Spectroscopy*, vol. 33, no. 1-2, pp. 49–61, 2003.

[44] C. James, A. A. Raj, R. Reghunathan, I. H. Joe, and V. S. Jayakumar, "Structural conformation and vibrational spectroscopic studies of 2,6-bis(*p*-*N*,*N*-dimethyl benzylidene) cyclohexanone using density functional theory," *Journal of Raman Spectroscopy*, vol. 37, no. 12, pp. 1381–1392, 2006.